Desalination and Water Treatment
www.deswater.com
33 (2011) 351–358
September
1944-3994 / 1944-3986 © 2011 Desalination Publications. All rights reserved.
doi: 10.5004/dwt.2011.2667

Effect of electric fields for reducing membrane fouling in dead-end filtration

Young G. Park

Department of Chemical Engineering, Daejin University, 11-1 Sundandong Pochunsi Gyungkido 487-711, Korea
Tel. +831-533-1970; Fax +831-536-6676; email: ypark@daejin.ac.kr

Received 30 November 2010; Accepted in revised form 27 March 2011

ABSTRACT

The purification of cell suspension in this presented work is to investigate in the membrane process under the influence of an electric field. This paper presents with example from membrane process showing how the filtration time is reduced by the use of an electric field. The transmembrane pressure (TMP) was reduced by 20% as the electric field increased. The concentration of biopolymers of cell suspension in the presence of an electric field was reduced by over 300% in comparison with the membrane process without an electric field. The hydraulic electrofiltration provides another substitute to the crossflow filtration in the purification of cell suspension.

Keywords: Protein; Electric field; Microfiltration

1. Introduction

The formation of a microbial cell layer (a filter cake) decreases the permeation flux in the crossflow filtration of microbial broths. In addition the decrease of the permeation flux is accelerates when the broth contains biopolymers and fine particles derived from medium components. We have shown that the cake layer of the fine particles or biopolymers formed additionally on the cake surface causes the increase in the resistance of the cake more than 10 times [1]. The resistance of the medium is also increased due to plugging of the membrane pores with the fine particles and biopolymers. The purification of cell suspension has been widely used in the electrodialysis, ultrafiltration, microfiltration when comparing with the number of studies on the use of conventional membrane for different cell suspensions' separation [2,3]. But they were not used as a purpose of enhancing the permeability. The newly developed techniques superimpose additional forces such as the pressured hydraulic force. Recently the dynamic filtration represents a further possibility for reducing the surface layer on the membrane of rotating disc filtration [2–4]. However, the principle disadvantage of this technique is that cannot be separated in high concentration of cell suspension. In this paper a superimposed another force, that is, an electric field induces as a force on charged particles in order to reduce the surface layer on the membrane. A newly developed type by an electric force has been invented a electro-microfiltration membrane [5,6]. Present studies in this article are experimentally to test the performance of new-typed electro-microfiltration membrane at a low hydraulic pressure and induces high amount of permeates. As such, the membrane filtration was investigated based on the membrane properties measured experimentally using the cake filtration theory [6]. The microfiltration technique was chosen to reduce the transmembrane pressure (TMP) and to increase the permeate flux. This study shows that this membrane system manufactured by a electro-microfiltration technique offers significant advantages.

Presented at the 3rd International Desalination Workshop (IDW 2010), November 3–6, 2010, Jeju, Korea
Organized by Center for Seawater Desalination Plant and European Desalination Society

2. Experimental methods

2.1. Permeability theory in porous membranes

A mathematical theory was derived for investigating the possible effect of forced intramembrane convection in a porous membrane. Since the flow velocity inside a porous membrane is governed by the Darcy's law

$$v = \frac{k}{\mu}\nabla P, \quad \nabla v = 0 \tag{1}$$

where k is the permeability; μ, the dynamic viscosity; and P, the pressure. v is the characteristic intramembrane flow velocity, and hence the parameter v can be defined by the pressure drop across the membrane ΔP. The mathematical description of the process is developed to relate the filtrate flow rate (q) to the pressure drop ($q = dV/dt$, where dV is the filtrate volume in time dt) as follows.

$$\frac{\Delta P}{L} = \frac{\mu}{kA}\frac{dV}{dt} \tag{2}$$

where L is the membrane thickness and A is the membrane area. During the filtration, the cake depth is assumed to increase due to the deposition of solids on the filter cake surface. The change in the cake depth is accompanied by changes in the fluid flow rate and pressure differential as the filtration time increases. Thus, Darcy's law contains a constant liquid viscosity (μ) and constant filter area (A). The uniform relation between the cake volume and the filtrate volume (V) has a constant of proportionality β, which can be used to give an equation for the cake depth (L_c):

$$L = \frac{\beta V}{A} \tag{3}$$

In Eq. (2), it is assumed that the pressure drop in the medium ΔP_m is added to the pressure drop over the filter cake ΔP_c to give the overall pressure drop.

$$\Delta P = \Delta P_c + \Delta P_m \tag{4}$$

If the cake resistance R_c is considered in Darcy's law, where $R_c = L_c/k_c$:

$$\Delta P_c = \mu R_c \frac{dV}{dt}\frac{1}{A} \tag{5}$$

Then the overall resistance to filtration increases with time due to the increase in the depth of the filter cake. However, the rate of increase in the filtration resistance is linear with respect to the mass of dry solids deposited per unit filter area. The cake thickness (L_c), solid density (ρ), and cake volume fraction (C) can be described by the following equation [4]:

$$\frac{dV}{dt} = \frac{A^2\Delta P}{\mu C V \alpha} \tag{6}$$

where α is $1/k_cC$, called the "specific resistance", which is composed of the cake permeability (k_c), cake volume fraction concentration (C) and solid density (μ). Eqs. (5) and (6) can be rewritten as substituting for Eq. (5) as follows.

$$\Delta P = \frac{\mu}{A}\left(R_c + R_m\right)\frac{dV}{dt} = \frac{\mu C\alpha}{A^2}V\frac{dV}{dt} + \frac{\mu}{A}R_m\frac{dV}{dt} \tag{7}$$

Eq. (7) is a straight line on a plot of filtration pressure against filtrate volume. Eq. (7) can be integrated using the limits: zero filtrate volume at zero time, V filtrate volume after time t, thus:

$$\frac{t}{V} = \frac{\mu\alpha C}{2\Delta P A^2}V + \frac{\mu R_m}{\Delta P\, A} \tag{8}$$

Eq. (8) is a straight line, where t/V is dependent and V is the independent variable. Thus a graph of the experimental data points of t/V against V permits calculation of the gradient and intercept of Eq.(8). The gradient and intercept are as follows:

$$\text{Gradient} = \frac{\mu\alpha C}{2\Delta P A^2}$$

$$\text{Intercept} = \frac{\mu R_m}{\Delta P A}$$

The permeability was measured in the pressure ranges of 1–10 kg_f/cm^2 using Eq. (7). The slope and intercept of Eq. (8) then estimated using the experimentally obtained data in order to estimate the permeabilities and the resistances.

3. Materials and methods

3.1. Materials

The composition of metabolites produced during fermentation is listed in Table 1. Amylase was purchased from Pacific Chemical (Seoul, Korea). The yeast was obtained from Mido Chemicals (Daeku, Korea) and the glucose levels were measured with a glucose card test strip (Arkaray, Japan). The crushed starch and plant-extract were used as the fermentation material for the purpose of producing different metabolites. The pH and glucose levels of the mixtures were measured every 12 h during the hydrolysis until the glucose level reached 5,000 mg/ml. The removal of particles from the crude broth was achieved centrifugation for 10 min at 1,000–4,000 rpm, using a Hanil Model centrifuger (Hail Science MF 80 Model, Korea). The analysis on the fermentation crude is listed in Table 1.

The solid contents from fermentation were removed by centrifugation and were used for all of the membrane studies. All the data pertaining to chemical constituents were collected during each batch fermentation run and was used to measure the overall performance of membrane separation. The chemical constituents of each of the

Table 1
Analysis on the fermentation broth

	Crude composition of fermentation broth
pH	6.4
Acid, % (v/v)	3.2
Latic acid, mg/L	3,345
Citric acid, mg/L	1,223
Amino acid, %(v/v)	1.29
Protein, mg/L	125.2

Table 2
Volatile compounds during fermentation (unit:peak area%)

Peak No.	Volatile compounds	Fermentation periods (d)			
		2	6	9	30
1	Ethyl acetate	7.93	2.90	0.56	5.12
2	1,1-diethoxy-ethane	—	—	—	0.53
3	1-chloro-pentane	—	—	—	14.87
4	Isobutyl alcohol	—	—	0.79	0.51
5	3-methyl-1-butanol	10.33	12.62	22.94	37.16
6	2-methyl-1-butanol	—	—	23.87	11.41
7	Methylbenzene	—	—	—	0.51
8	hexamethyl-cyclotrisiloxane	0.23	0.21	0.41	045
9	Methyl-cyclopentane	0.12	034	0.41	2.30
10	Ethyl caproate	5.31	0.76	4.40	3.37
11	dl-limonene	—	—	—	0.50
12	2,2-dimethyl-1,3-propanediol	1.69	1.89	2.34	3.45
13	3-methylbutyrate	0.37	—	—	—
14	Isoamyl acetate	21.21	1.12	1.11	2.10
15	2-methyl-1-butyl acetate	6.12	6.34	7.12	7.78
16	2-ethyl-1-hexanol	2.52	1.14	2.56	3.21
17	Phenylethyl alcohol	7.06	3.87	16.31	29.34
18	Dedamethyl-cyclopentasiloxane	0.11	0.20	0.70	0.83
19	Ethyl caprylate	2.27	0.36	6.21	3.40
20	Phenethyl acetate	0.1	0.20	0.23	0.26
21	Ethyl pelargonate	—	—	—	0.65
22	Ethyl caprate	—	—	0.40	1.90
23	4-methyl-2,6-di-tert-butylphenol	0.28	1.13	2.12	2.90
24	N-(2-phenylethyl)acetamide	1.94	1.93	2.01	2.23
25	Ethyl palmitate	0.07	—	—	—
26	Dibutyl phthalate	—	—	0.57	1.12
27	Eicosane	9.13	9.63	9.65	9.69
28	1-hentetracontanol	4.46	4.59	4.90	5.23
29	Heneicosane	0.21	0.49	1.12	1.23

fermentation, as measured by the chromatogram peak, could be obtained by cell metabolism inside the yeast cell (Table 2). The cellular concentration was 0.05–0.2 g/L.

As predicted, the pyruvate pathway leads to the synthesis of isoleucine, valine, phenylalanine, tryptophan and leucine (Fig. 1a). Fusel alcohol is produced by the metabolism of these amino acids inside the cell membrane (Fig. 1b). The metabolically produced fusel alcohol can be significantly adjusted according to the fermentation method and type of raw material. The chemical compositions fermented by the 1:1 mixture were measured by GC-MS (Table 2). The constituent chemicals resulted in 6 alcohol compounds (59.31%), 7 ester compounds (29.93%), acid compounds (5.08%) and phenol (0.49%). The representative chemicals recovered and separated using the membrane process were acetic acid, ethyl ester, 3-methyl-1-butanol (isoamyl alcohol), amino acids and proteins. Protein concentration was measured using the Bradford assay.

3.2. Membrane and experiment apparatus

The membranes used in the present study were materials provided by Millipore (USA). They had pore sizes of 0.22 μm – 3.5 μm and had 47 mm diameter-dimension. Membranes were prepared from polyvinylidene fluoride membrane made by the so-called phase inversion technique and they were hydrophilic and hydrophobic in nature. To compare the permeate flux of the polyvinylidene fluoride membrane, three other kinds of membrane were also used: hydrophobic and hydrophilic polyvinylidene fluoride membranes of three different pore-sizes (0.22 μm, 0.46 μm, 2.5 μm). These MF membranes were purchased from Millipore (Bedford MA, USA). Microfiltration experiments were performed with a laboratory-sized plant. The experiments were carried out using a conventional microfiltration pilot as shown in Fig. 1. The flow rate was maintained using a centrifugal pump and determined by a flowmeter. The measuring process required the use of a rigid plate-frame membrane device with an external skin and was indicated by the average value of the manometers. The electro-microfiltration apparatus was made by Teflon material for the prevention of an electric conductivity and had pressure ranges between 0 and 10 kg_f/cm^2. Masterflex Easy-Load model (7518-00, USA) was used as the hydraulic pump and controlled the permeate flux. The experimental apparatus used in this work is shown in Fig. 1. The filtration area of membrane was 17.3 cm^2: three new membrane segments, hold in a polyvinyl carbonate device, were used for each experiment. The operating conditions were: filtered volume 12,500–13,000 ml, mean tangential flow velocity 2 cm/s, temperature 20°C and the flow circuit was constructed entirely of stainless steel. Pumping was provided by means of a variable speed gear pump, providing low shear to avoid denaturation of protein. Transmembrane

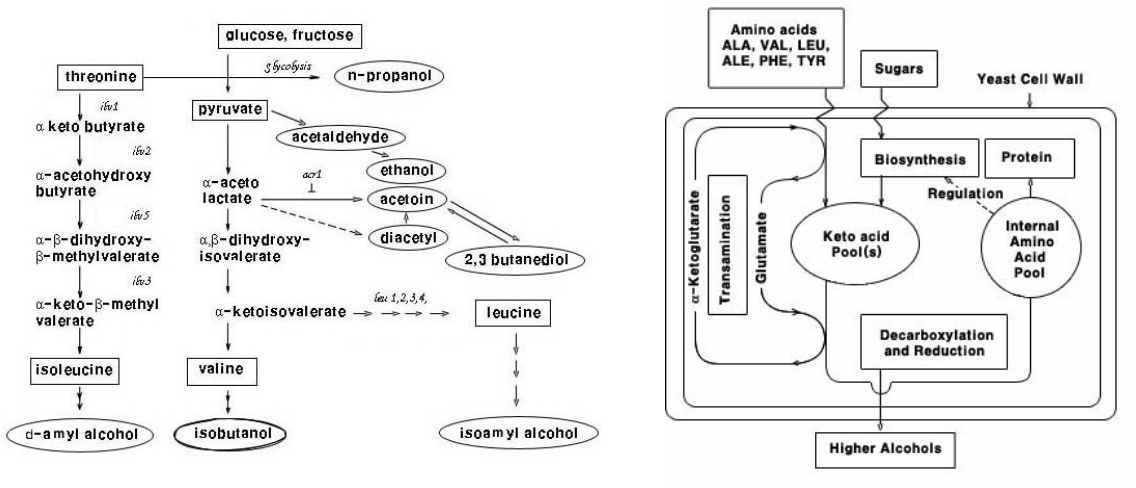

Fig. 1. A schematic diagram of metabolic pathways, (a) pyruvate metabolic pathway, (b) fusel alcohol synthesis pathway.

pressure (TMP) was adjusted to 10 kg_f/cm^2. The permeation flux was determined by weighing and timing. At the beginning of each microfiltration experiment, the protein solution was filtered on the new membrane until the flux has reached a constant value. The filtration area of membrane was 17.3 cm^2: three new membrane segments, hold in a polyvinyl carbonate device, were used for each experiment. The operating conditions were: filtered volume 125–3,000 ml, mean tangential flow velocity 2 cm/s, temperature 20°C and the flow circuit was constructed entirely of stainless steel. Pumping was provided by means of a variable speed gear pump, providing low shear to avoid denaturation of protein. Transmembrane pressure (TMP) was adjusted to 10 kg_f/cm^2. The permeation flux was determined by weighing and timing. At the beginning of each microfiltration experiment, the protein solution was filtered on the new membrane until the flux has reached a constant value. The rejection coefficient is 1 minus the ratio of the concentration of the protein in the permeate to the concentration of protein in the bulk feed to the module. The medium resistance is obtained by applying cumulative volume by time to the initial stages of filtration using Eq. (1).

$$R_m = \frac{A\Delta P}{\mu\left(\frac{dV}{dt}\right)_{t=0}} \tag{9}$$

3.3. Membrane and microfiltration experiments

The membranes used in the present study were 47 mm with pore sizes ranging from 0.45 μm–5.0 μm (Millipore, USA), which were prepared from a polyvinylidene fluoride using the phase inversion technique. Microfiltration experiments in the pilot plant were performed at an input capacity of 10 L/h. The membrane purification apparatus was made of stainless steel and had pressure ranges between 0 and 10 kg_f/cm^2. The masterflex Easy-Load model (MasterFlex 7518-00, USA) was used as the hydraulic pump and controlled the permeate flux (Fig. 2). The filtration area was 17.3 cm^2 with three new membrane segments held in a polyvinyl carbonate device for the experi-

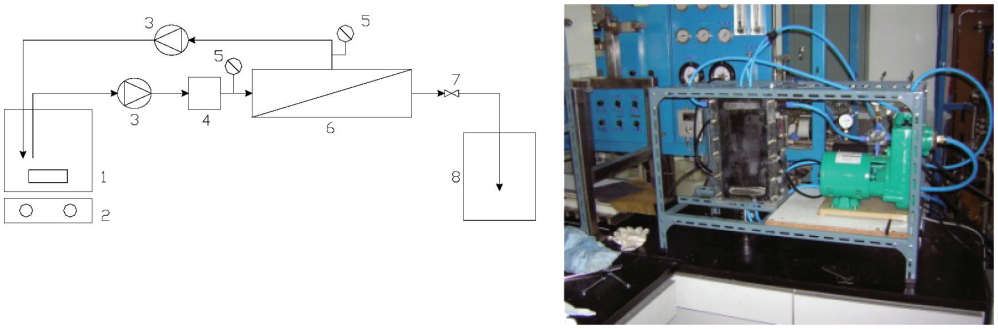

Fig. 2. Schematic diagram of pilot plant (left), 1.electric power unit, 2: control box, 3: peristatic pump, 4: mixing tank, 5: metering pressure-gauge, 6: membrane apparatus, 7: on-off valve, 8: permeate collecting tank; Pilot plant picture (right).

ment. The operating conditions were: a filtered volume 700 ml with a mean tangential flow velocity 2 cm/s and a temperature of 20°C. The flow circuit was constructed entirely of stainless steel and pumping was achieved by means of a variable speed gear pump which provides low shear to avoid the denaturation of amino acids. The transmembrane pressure was adjusted to 10 kg_f/cm^2 and the permeation flux was determined by weighing and timing. At the beginning of each microfiltration experiment, the broth was filtered on the new membrane until the flux has reached a constant level. The concentration of the protein was measured by the Bradford method, using a kit supplied by Bio-Rad Lab. (New Jergy, USA).

4. Results and discussion

4.1. Effect of hydraulic force on microfiltration

As already discussed previously and in accordance with other works, the protein in the suspension took a determinant part in cake formation. For example, initial fouling rates were significantly decreased while volumetric flow rate increased. When the pump delivered a uniform volume of influent into the membrane, the microfiltration rate remained constant while filtering incompressible material. However, to achieve this constant rate, the pressure delivered had to be increased by 3.5 kg_f/cm^2 to overcome the increasing resistance to filtration caused by the cake deposition. A constant rate filtration was easily observed on the plot of the filtrate volume using the protein solution relative to time. Fig. 3 shows a graph where the plot of the volume filtrate collected against the filtration time produced a linear line, all the filter forms in Fig. 3 displayed some form of compressibility in practice; increasing the filtration pressure resulted in an increased filtration time.

Recently, conventional cake filtration based on Darcy's law has been applied for the description of dead-end filtration. For a global view of the cake filtration Darcy's law can be written as

$$\frac{t}{V} = \frac{\mu \alpha m}{2\Delta P A^2} \tag{10}$$

A plot of the filtration volume against the filtrate time linearly increased as shown in Fig. 3. A suitable rearrangement of the gradient coupled with the initial values taken from the graph provided values for the medium resistances as shown in Eq. (6). The slopes in Fig. 3 for the microfiltration depending upon hydraulic pressures of 2, 2.5, 2.8 and 3.1 kg_f/cm^2 had values of 0.61, 1.27, 1.28 and 1.61 respectively, which permeated more than 200% in comparison with the highest hydraulic pressure of 3.1 kg_f/cm^2.

The most economic way of removing liquid from an incompressible filter cake is to filter at the lowest pressure required to overcome the fluid drag within the cake. But

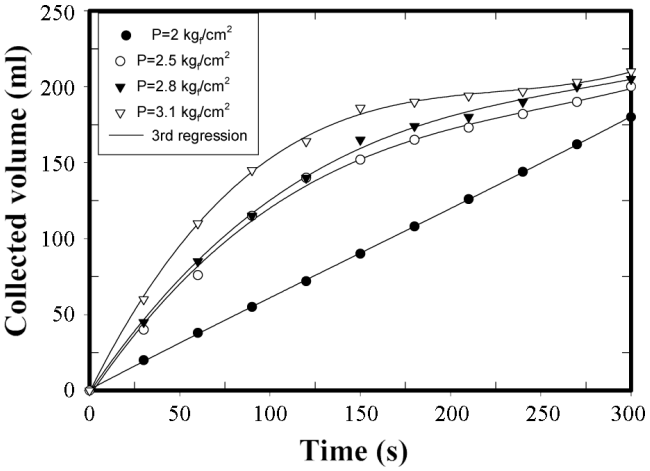

Fig. 3. Permeate rate filtration in different hydraulic pressures.

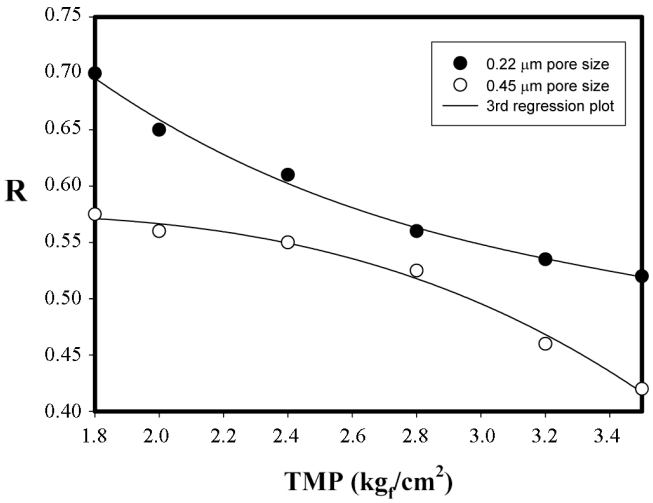

Fig. 4. Rejection efficiencies by trans-membrane pressure in different pore-sized membranes.

the filter cake contributed to decrease the concentration of the protein. The overall removal efficiencies during microfiltration of pore sizes of 0.22 μm and 0.45 μm had 63.5% and 59.6% in case of protein. But the removal efficiencies were significantly different depending upon the pore sizes of membranes as shown in Fig. 4. When the TMP increased, some aggregated organic matter deposited on the membrane front face, but this deposition remained insufficient to lead to a full coverage of the surface. The membrane experiment shows that the permeate rate was difficult to penetrate in the membrane having 0.22 μm pore size. Fig. 4 shows that the rejection efficient can be significantly varied depending upon TMP and pore size of membrane. The rejection efficiencies in the cross-flow membrane decreased more with the increase of TMP, these efficiencies were showing much differently depend-

ing upon the pore size of membrane. As TMP increased from 1.8 kg_f/cm^2 to 3.5 kg_f/cm^2, the rejection efficiencies were decreased 25.0% in the membrane of 0.22 μm and were done 27.1% in the membrane of 0.45 μm. For example, the rejection efficiencies in the 0.22 μm membrane were 0.7 at 1.8 kg_f/cm^2 and 0.525 at 3.5 kg_f/cm^2, but those in the 0.45 μm membrane were 0.576 at 1.8 kg_f/cm^2 and 0.425 at 3.5 kg_f/cm^2.

4.2. Effects of membrane pore-size and cellular concentration during electro-microfiltration

Fig. 5 shows the differences of collected in the hydraulic pressure in relation to the filtration time as a function of electric field at an applied pressure of 2 kg_f/cm^2. The pressure electro-microfiltration provides more filtration for protein purification. The applied electric field strength was 9 V–15 V. In this experiment hydraulic pressure was also applied over 2 kg_f/cm^2. It is apparent that there is a retentate layer on the anode-side membrane, while on the cathode-side membrane there is permeate layer which is almost clear. If the hydraulic pressure is increased, the highly compressible protein' layers are compressed. This leads to the effect that an electric field acts along the cake layer. As the electric field is greater, the protein's migration has increased. So the electric field and therewith the electrophoretic velocity of the constituents close to the cathode-side membrane is reduced at smaller total concentrations than in electro-filtrations with higher pressure.

As an electric field increased, the permeate rate was also increased depending upon the size of an electric field. As a result, the permeate velocities were increased by 118.7% and 126.1% in the membrane of 0.45 μm pore size and done by 99.0% and 118.7% in the membrane of 0.22 μm pore size as electric field was increased as 9 V and 15 V respectively as shown in Fig. 5. This indicates that the permeate velocity increased to the direction of an electric field and the amount of permeate also increased. Therefore, the rejection efficiencies significantly decreased as an electric field increased as shown in Fig. 5. Fig. 6 shows that the TMP was significantly decreased as an electric field increased. For example, the differences of TMP were approximately 20% in the pore sizes between 0.22 μm and 0.45 μm respectively. Also, the TMP was significantly varied depending upon protein concentration. As the cellular concentration increased four times from 0.05 g/L to 0.2 g/L, the TMP was approximately decreased by 20% as shown in Fig. 6.

The amount of permeation with the micro-electrofiltration membrane was above six times greater than that with the microfiltration membrane as shown in Fig. 6. All the experimental results in Fig. 6 show a very good linearity, meaning that the rate of permeation remained constant. The amounts of the permeation of 0.05 g/L celluar concentration were increased by 334% as the pore sizes of membrane were increased from 0.22 μm to 2.5 μm. But when an applied electric field was 15 V, The amounts of the permeation of 0.05 g/L cellular concentration were increased by 246% when the pore sizes of membrane were from 0.22 μm to 2.5 μm. But as the cellular concentration increased to 0.2 g/L, the amount of permeation in the electro-microfiltration membrane was also about five times greater than that with the microfiltration membrane as shown in Fig. 6. This indicates that the electric field induces the enhancement of permeation rate in the membrane. By the same previous procedure, the amounts of the permeation in cases of 0.05 g/L and 0.2 g/L cellular concentration in the presence of an electric field were increased by 762%, 544%, 555% and 160%, 435%, 449% in comparison with the absence of an electric field as the pore sizes of membrane were increased 0.22 μm, 0.45 μm

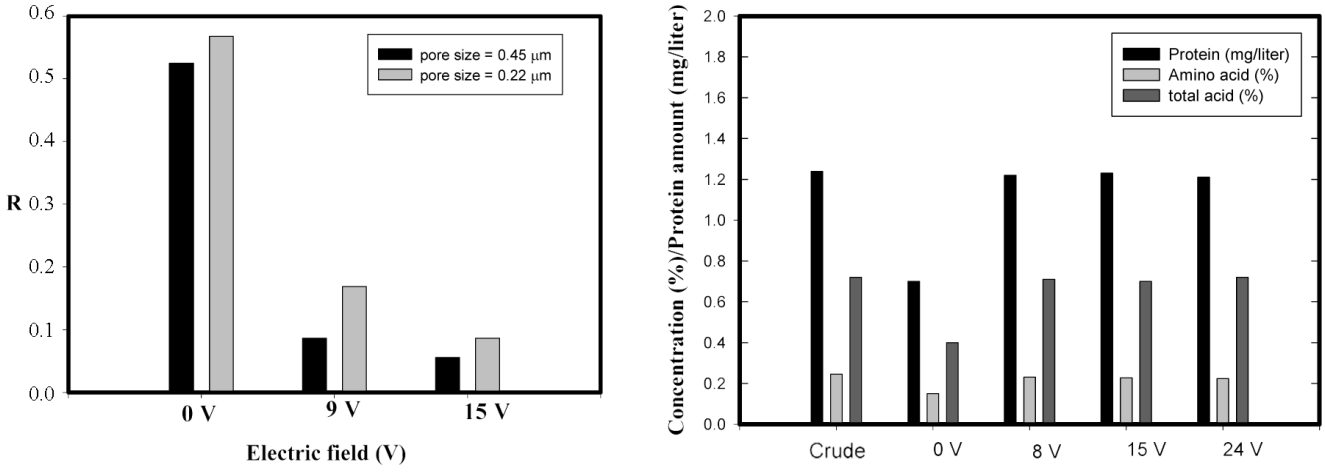

Fig. 5. Rejection efficiencies by electric fields in different pore-sized membranes (left), Electric field effects of protein purification (right).

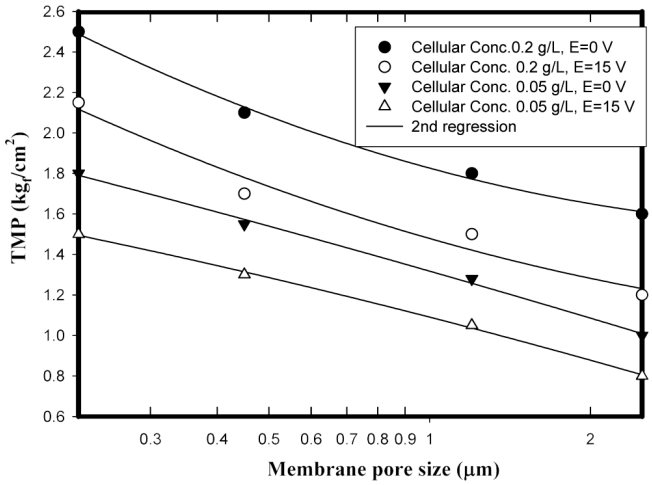

Fig. 6. Variation of transmembrane pressure with different membrane pore sizes.

and 2.5 μm. This indicates that the permeation rate by an electric field greatly increased in more porous membrane.

4.3. Effects of pressure electro-microfiltration

In electrofiltration an electric fieldis superimposed on a traditional pressure filtration set-up. This electric field acts parallel to the flow direction of the filtrate. Due to the electrophoretic migration of the charged protein away from the membrane, the assembly of a surface layer on the membrane may be reduced. In addition the migration of the counter ion atmosphere around the charged proteins leads to an electro-osmotic dewatering. Park et al. [10] modified Darcy's law to account for the electrophoretic and the electro-osmotic effect:

$$\frac{t}{V} = \frac{\mu\alpha C\left(1-\frac{E}{E_{cr}}\right)m}{2\left(\Delta P_H - \Delta P_E\right)A^2} \tag{11}$$

where ΔP_E is the electro-osmotic pressure, E is the electric field strength and E_{cr} is the critical electric field strength.

Fig. 7 shows that the permeate rate in the electro-microfiltration membrane can be enhanced by hydraulic pressure in the membrane since the electric field increased from 3 V to 24 V (3 V, 9 V, 15 V and 12 V). When the hydraulic pressure was 1.3 kg$_f$/cm^2, the permeate rates were not different even though the electric field varied. This indicates that an electric field did not exclusively play a role to enhance the permeability. But as the hydraulic pressure increased with applied electric field, the permeate rates significantly increased. For example, the permeate rate were 269%, 274%, 295% and 327% as an electric field increased from 3 V, 9 V, 15 V and 24 V respectively when the hydraulic pressure is 2.1 kg$_f$/cm^2 in comparisons with the hydraulic pressure of 1.3 kg$_f$/cm^2.

This indicates that the permeate rate in the electro-microfiltration membrane is enhanced by the hydraulic pressure with an electric field. In cases of the hydraulic pressure of 2.8 kg$_f$/cm^2 and 3.5 kg$_f$/cm^2, the permeate rates were 362%, 476%, 490%, 500% and 394%, 530%, 554%, 568% as an electric field increased from 3 V, 9 V, 15 V and 24 V respectively in comparisons with the hydraulic pressure of 1.3 kg$_f$/cm^2. Therefore, the permeate rate in the pressure electro-microfiltration followed to Eq. (10) that the permeation rate linearly increased with hydraulic pressure and electric field.

5. Conclusions

The microfiltration was found to provide a fairly rigid

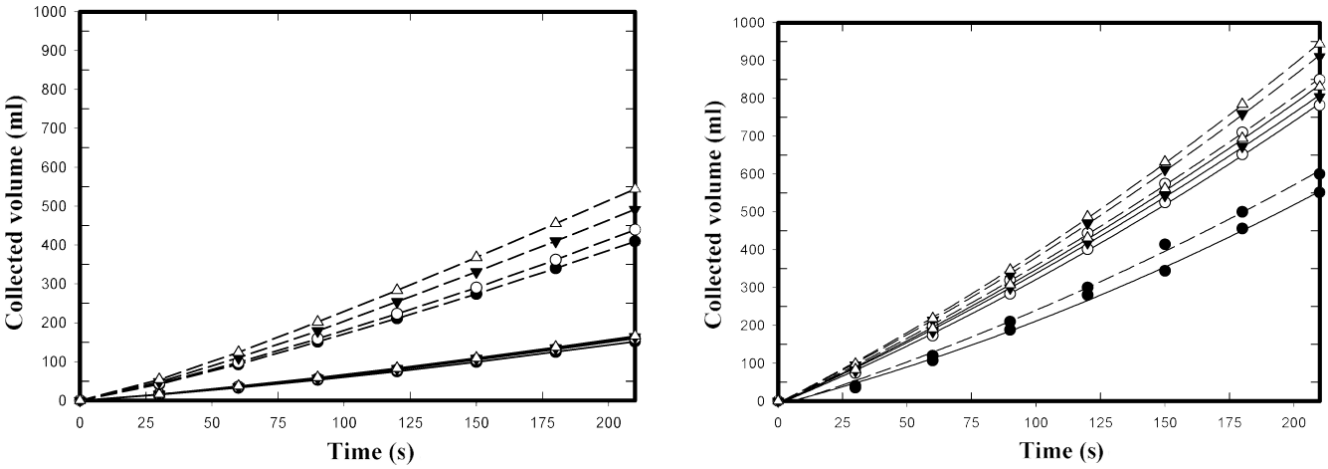

Fig. 7. Effects of hydraulic pressure in the pressure electrofiltration. (a) Effects of low hydraulic pressure in the pressure electrofiltration: (—) hydraulic pressure of 1.3 kg$_f$/cm^2, (- - -) hydraulic pressure of 2.1 kg$_f$/cm^2; (b) Effects of high hydraulic pressure in the pressure electrofiltration: (—) hydraulic pressure of 2.8 kg$_f$/cm^2, (- - -) hydraulic pressure of 3.5 kg$_f$/cm^2.

support based on the electric field. The pressure electro-filtration designed by a hydraulic pressure enhanced the permeability of the influent. The permeability of protein was proportional to hydraulic pressure with an electric field, indicating that the protein quickly orients in the field direction through the membrane pores. The conventional filtration theory showed the electro-microfiltration membrane to be superior to the microfiltration membrane. The experimental results can be described as follows.

First, the transmembrane pressure was lowered in the electro-microfiltration membrane by 20% in comparison with the conventional microfiltration membrane.

Second, the permeate rate of the electro-microfiltration membrane had over 200% higher than the conventional microfiltration membrane.

Third, the membrane resistance (R_m) in the pore-filled membrane was significantly reduced by 500% in comparison with the conventional microfiltration membrane and resistance in the cake layer was reduced by 16%.

Fourth, TMP was approximately decreased by 20% as the cellular concentration increased four times from 0.05 g/L to 0.2 g/L.

Fifth, the amount of hemoglobin was significantly reduced by 45% in the microfiltration in the absence of an electric field. The concentrations of protein maintained equal amounts during the electro-microfiltration. Therefore, it is important for the electro-microfiltration membrane to play a significant role in the transport of the protein in the membrane process.

Accordingly, since the membrane was artificially provided with new technology of membrane process, the present study experimentally demonstrates that the permeability inside a membrane can be controlled using an electric field.

Acknowledgement

We are thankful that this work was supported by the Daejin University Special Research Grants in 2011.

References

[1] Y. Park, The effect of porosity of sieving particles on the removal efficiency of organic substances via biofilter in the fixed bed. Biotechnol. Bioprocess Eng., 7 (2002) 31–37.
[2] D. Krstic, S. Markov and M. Tekic, Membrane fouling during cross-flow microfiltration of polyporous squamosus fermentation broth. Biochem, Eng. J., 9 (2001) 103–109.
[3] T. Tanaka, Y. Yamagiwa, T. Nagano, M. Taniguchi and K. Nakanishi, Relationship between cake structure and membrane pore size in crossflow filtration of microbial cell suspension containing fine particles. J. Chem. Eng. Japan, 34 (2001) 1524–1531.
[4] J. Engler and M. Wiesner, Particle fouling of a rotating membrane disk. Wat. Res., 34 (1999) 557–565.
[5] C. Serra, M. Wiesner and J. Laîné, Rotating membrane disk filters: design evaluation using computational fluid dynamics. Chem. Eng, Sci., 72 (1999) 1–17.
[6] U. Holeschovsky and C. Cooney, Quantitative description of ultrafiltration in a rotating filtration device. AIChE J., 37 (1991) 1219–1226.
[7] Z. Lararova and W. Serro, Electromembrane separation of mineral suspensions: Influence of process parameters. Separ. Sci. Technol., 37 (2002) 515–534.
[8] S. Galier and H. Balmann, Study of the mass transfer phenomena involved in an electrophoretic membrane contactor. J. Membr. Sci., 194 (2001) 117–133.
[9] C. Byers and A. Amarnath, Understand the potential of electro-separation. Chem. Eng. Progress, February (1995) 63–69.
[10] Y. Park and H. Byun, Application of the cake-filtration theory to analyze the permeate performance in poly(vinylbenzyl chloride)-filled microfiltration membrane. J. Ind. Eng. Chem., 8 (2002) 537–545.